



Supplementary Information for

Propofol disrupts alpha dynamics in functionally distinct thalamocortical networks during loss of consciousness

Veronica S. Weiner^{1,2+}, David W. Zhou^{1,2,3,4+▲}, Pegah Kahali^{2,3+◇}, Emily P. Stephen^{2★}, Robert A. Peterfreund^{3,5}, Linda S. Aglio^{5,6}, Michele D. Szabo³, Emad N. Eskandar^{5,7†}, Andrés F. Salazar-Gomez^{3⊙}, Aaron L. Sampson^{3▪}, Sydney S. Cash^{4,5}, Emery N. Brown^{1,2,3,5,8,9}, Patrick L. Purdon^{3,5}

¹Department of Brain and Cognitive Sciences, Massachusetts Institute of Technology, Cambridge, MA, USA

²Picower Institute for Learning and Memory, Massachusetts Institute of Technology, Cambridge, MA, USA

³Department of Anesthesia, Critical Care and Pain Medicine, Massachusetts General Hospital, Boston, MA, USA

⁴Center for Neurotechnology and Recovery, Department of Neurology, Massachusetts General Hospital, Boston, MA, USA

⁵Harvard Medical School, Boston, MA, USA

⁶Department of Anesthesiology, Perioperative and Pain Medicine, Brigham and Women's Hospital, Boston, MA, USA

⁷Department of Neurological Surgery, Massachusetts General Hospital, Boston, MA, USA

⁸Division of Health Sciences and Technology, Harvard Medical School/Massachusetts Institute of Technology, Cambridge, MA, USA

⁹Institute of Medical Engineering and Sciences, Massachusetts Institute of Technology, Cambridge, MA, USA

▲Present address: Carney Institute for Brain Science, Brown University, Providence, RI, USA

◇Present address: Department of Neurology, Keck Medical Center, University of Southern California, Los Angeles, CA, USA

★Present address: Department of Math and Statistics, Boston University, Boston, MA, USA

†Present address: Department of Neurological Surgery, Albert Einstein College of Medicine—Montefiore Medical Center, Bronx, NY, USA

⊙Present address: Open Learning, Massachusetts Institute of Technology, Cambridge, MA, USA

▪Present address: Zanvyl Krieger Mind/Brain Institute, Johns Hopkins University, Baltimore, MD, USA

+Equal contribution

✉Correspondence: David W. Zhou, Patrick L. Purdon
dwzhou@alum.mit.edu, patrick.purdon@mgh.harvard.edu

This PDF file includes:

Supplementary Tables 1-4
Supplementary Figures 1-6
Data Materials and Availability

Supplementary Tables and Figures

Supplementary Table 1. Patient demographic and clinical information.

Subject	Age / gender / weight, kg	Total # implanted channels	# of implanted channels analyzed	# of intracranial channels removed	Number and type of channels analyzed	Lengths of recordings, in seconds (time preceding LOC)	Anesthetic agents given prior to end of post-LOC epoch	Basis of LOC definition
S1	21 / M / 91*	72	72	0	Five strips (16x4, 8x1)	2031.56 (1875.33)	Propofol, fentanyl	Auditory task / LR-FNR**
S2	24 / F / NA***	72	68	4	Two depths (8x2), four strips (32x1, 8x1, 6x2)	1251.88 (671.11)	Propofol	Auditory task / LR-FNR
S3	31 / F / 63	34	34	0	Five depths (6x3, 8x2)	1488 (648.06)	Propofol	Auditory task / LR-FNR
S4	45 / F / 98	40	39	1	Five depths (8x4, 7x1)	934 (514.16)	Propofol, fentanyl, sevoflurane, nitrous oxide	Auditory task / LR-FNR
S5	22 / M / 65	124	119	5	Five depths (8x5), one grid (60), four strips (8x1, 4x3)	970.08 (379.08)	Propofol, fentanyl, isoflurane, nitrous oxide	Auditory task / LR-FNR
S6	52 / F / 65	96	92	4	Two depths (8x2), one grid (61), four strips (4x3, 3x1)	2659.60 (2106.19)	Propofol, fentanyl	Auditory task / LR-FNR
S7	19 / M / 70	112	111	1	Four depths (8x2, 6x2), one grid (64), four strips (4x2, 3x1)	1435 (847.18)	Propofol, remifentanyl	Auditory task / LR-FNR
S8	29 / M / 136	80	75	5	Ten depths (8x6, 7x3, 6x1)	1461.70 (970)	Propofol, fentanyl, desflurane	Auditory task / LR-FNR
S9	35 / M / 73	80	75	5	Ten depths (8x5, 7x5)	737.05 (462)	Propofol	Did not participate / Bolus + 15 seconds
S10	32 / M / 67	112	112	0	Four depths (8x4), one grid (64), three strips (8x1, 4x2)	831.86 (380)	Propofol, nitrous oxide	Did not participate / Bolus + 15 seconds
S11	23 / F / 59	100	100	0	Three depths (8x1, 6x2), one grid (64), four strips (4x3)	819.66 (395.14)	Propofol, fentanyl	Auditory task / LR-FNR

* weight taken after surgery date

** LR-FNR = Halfway between last response and first non-response to behavioral task

*** NA = Not available

Supplementary Table 2. Patient-specific analysis metadata.

Subject	Length of pre-LOC coherence analysis epochs in seconds	Length of post-LOC coherence analysis epochs in seconds	Percent variance explained in top three pre-LOC principal component (bootstrap median, IQR)	Percent variance explained in top three post-LOC principal component (bootstrap median, IQR)
S1	345.77	71.97	38.87, 2.43	55.26, 21.41
S2	150.00	419.00	42.47, 2.33	40.12, 1.22
S3	461.46	118.90	71.56, 1.37	68.74, 2.31
S4	503.17	100.00	63.75, 1.36	78.23, 5.47
S5	258.08	190.80	38.26, 2.753	33.00, 2.60
S6	150.00	103.80	23.26, 1.50	20.9, 1.18
S7	100.00	475.91	28.56, 1.53	23.10, 0.98
S8	410.80	324.30	38.97, 1.79	54.74, 1.87
S9	377.90	197.80	46.39, 1.40	76.41, 2.50
S10	44.20	150.00	42.41, 14.08	54.35, 6.20
S11	195.14	101.00	19.57, 0.76	29.79, 1.59

Supplementary Table 3. Categorization of structural regions and labels

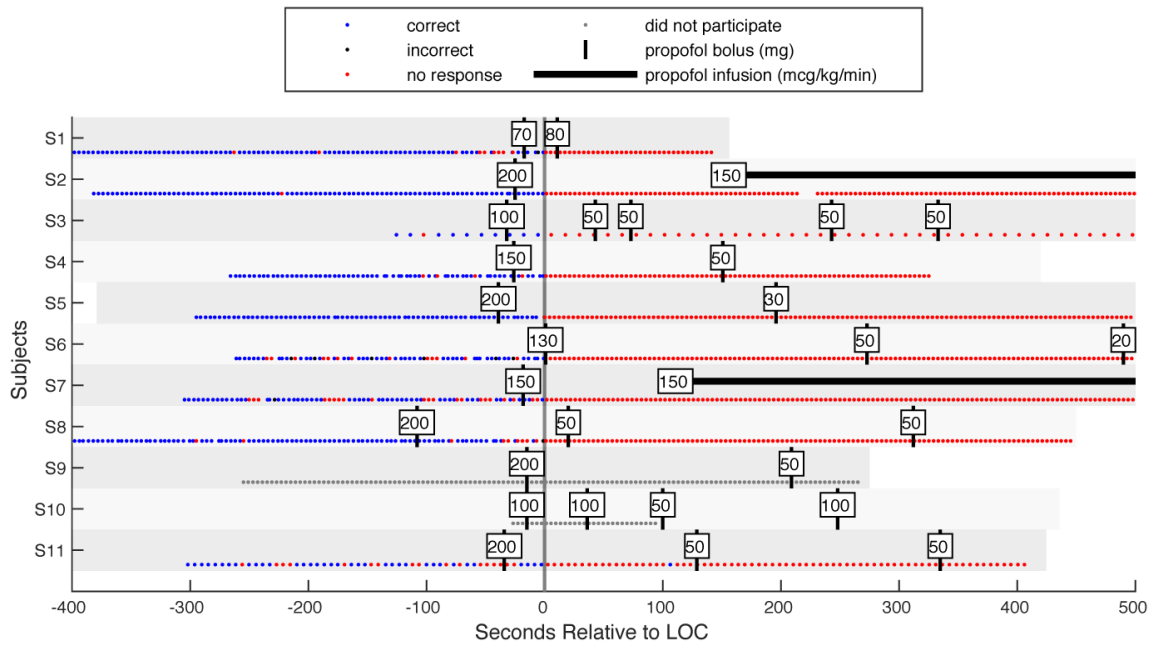
Structural region category	Freesurfer structural labels
anterior cingulate	rostral anterior, caudal anterior
posterior + isthmus of cingulate	posterior gyri, isthmus of
superior frontal + pole	frontal pole and superior frontal gyrus
orbitofrontal	medial and lateral orbitofrontal cortex
inferior frontal	pars orbitalis, pars opercularis, pars triangularis
precentral	precentral gyrus
middle frontal	middle frontal gyrus
medial temporal + pole	temporal pole, hippocampus, parahippocampal, entorhinal cortices
inferior temporal	inferior temporal gyrus
superior temporal	superior temporal gyrus
parietal	superior and inferior parietal lobules
middle temporal	middle temporal gyrus
postcentral	postcentral gyrus
occipital	superior occipital cortex, precuneus, pericalcarine, fusiform, lingual gyri

Supplementary Table 4. Human Connectome Project matches

Subject	Human Connectome Project matched subject IDs
S1	107422, 187850, 573451
S2	140925, 480141, 565452
S3	136732, 175237, 406836
S4	202820, 757764, 905147
S5	107422, 187850, 573451
S6	202820, 757764, 905147
S7	107422, 187850, 573451
S8	346137, 594156, 958976
S9	108222, 540436, 592455
S10	173738, 397861, 818455
S11	205725, 706040, 877269

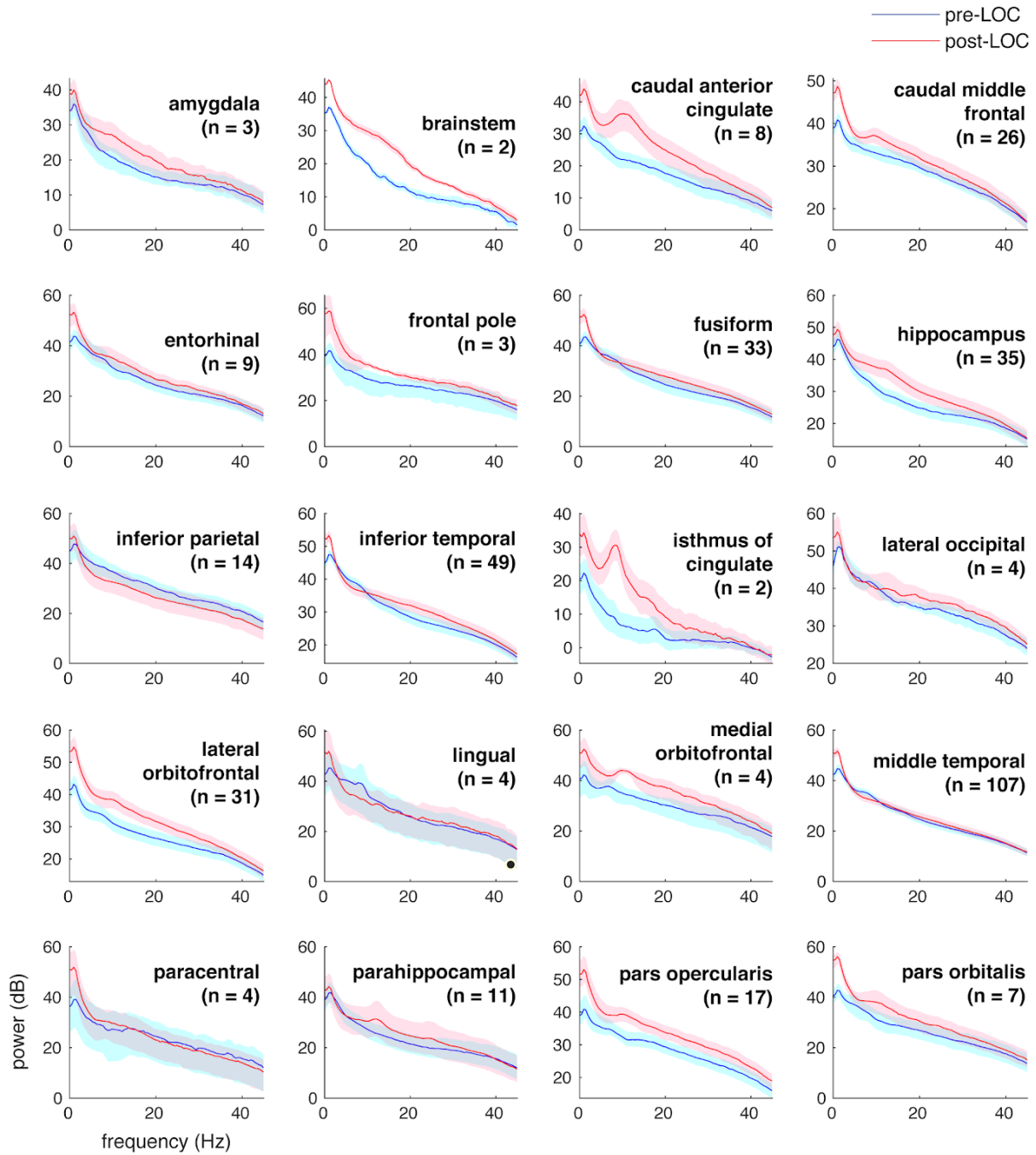
Supplementary Figure 1. Patient anesthesia administration time courses

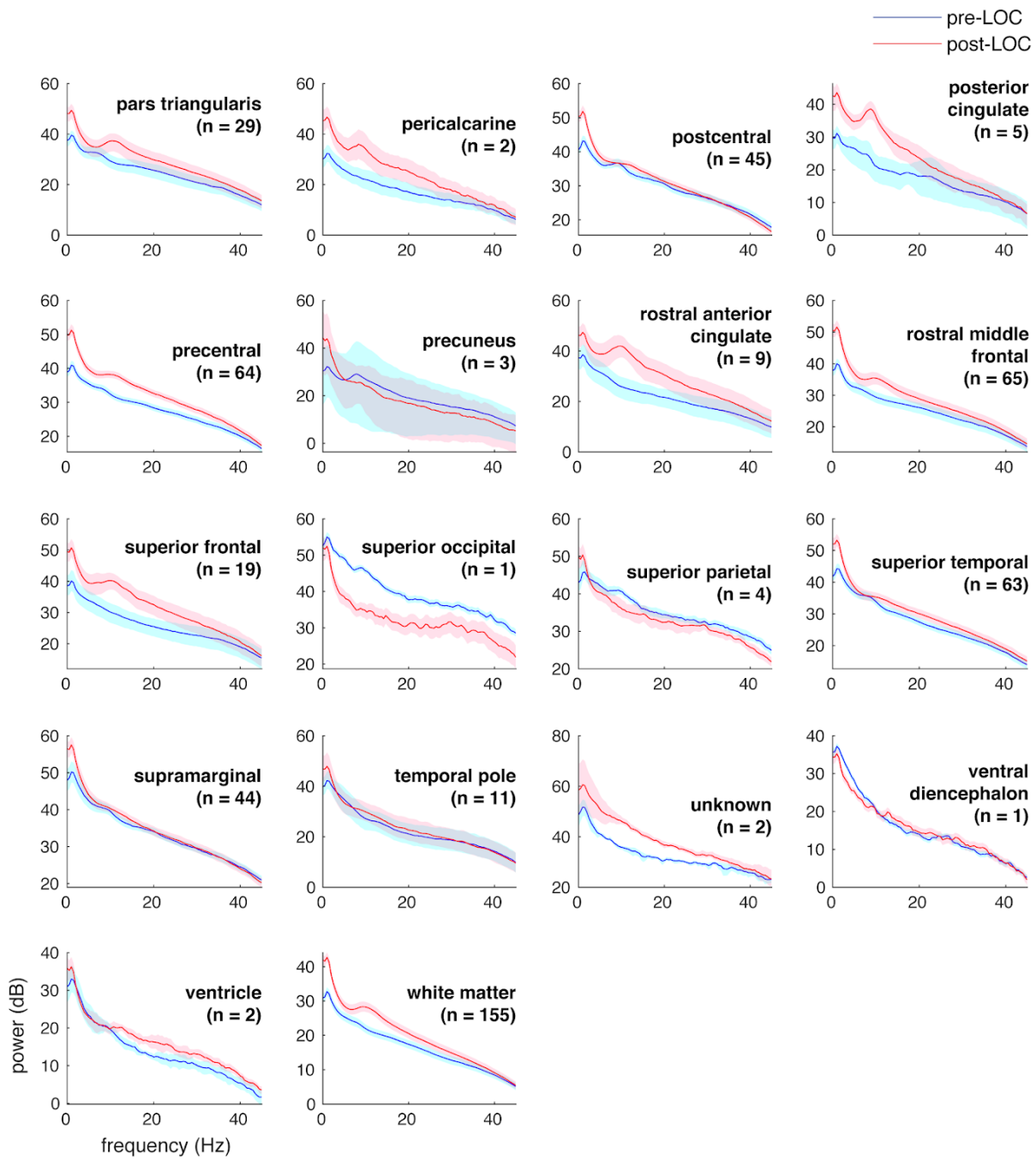
Shaded gray rows cover the start to end of each recording. Two patients did not participate in the behavioral paradigm, due to either failure to execute the task or exclusion at the request of the clinician. For these two patients, LOC was marked at 15 seconds after first propofol bolus injection.



Supplementary Figure 2. Pre- and post-LOC spectra across recorded regions.

Pre- and post-LOC multitaper spectra from all anatomical regions that contained implanted channels. Shaded boundaries represent the 95% bootstrap standard error of the mean.

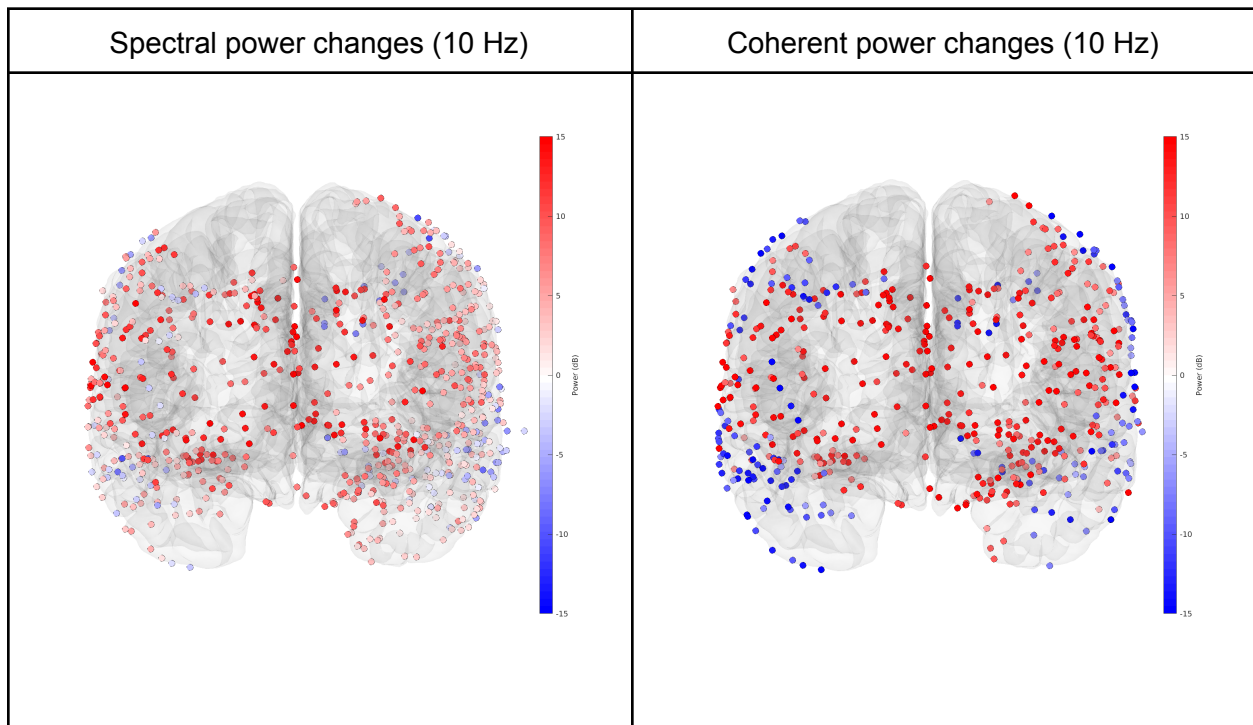


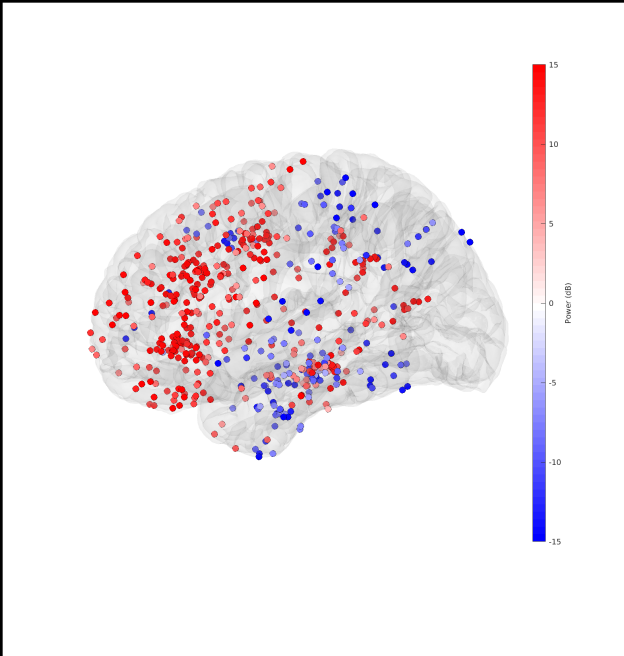
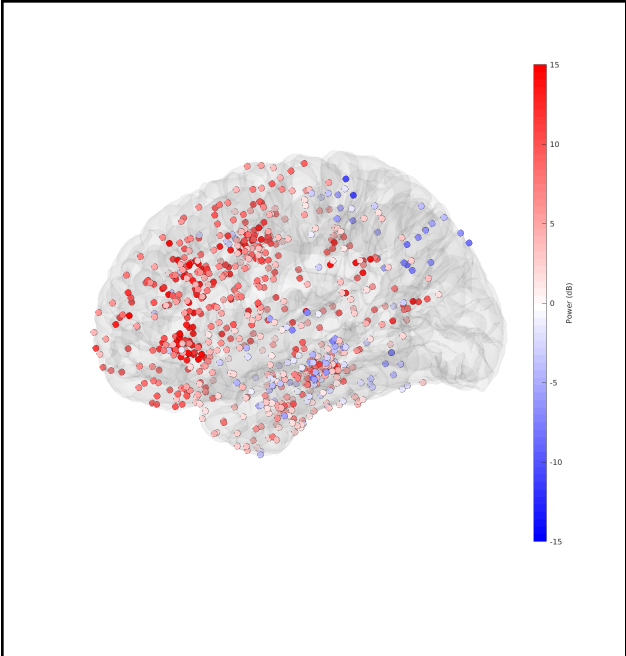
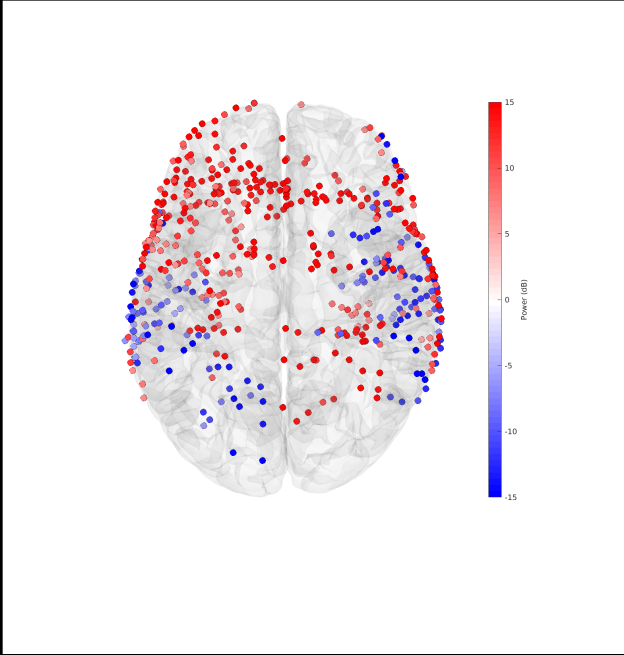
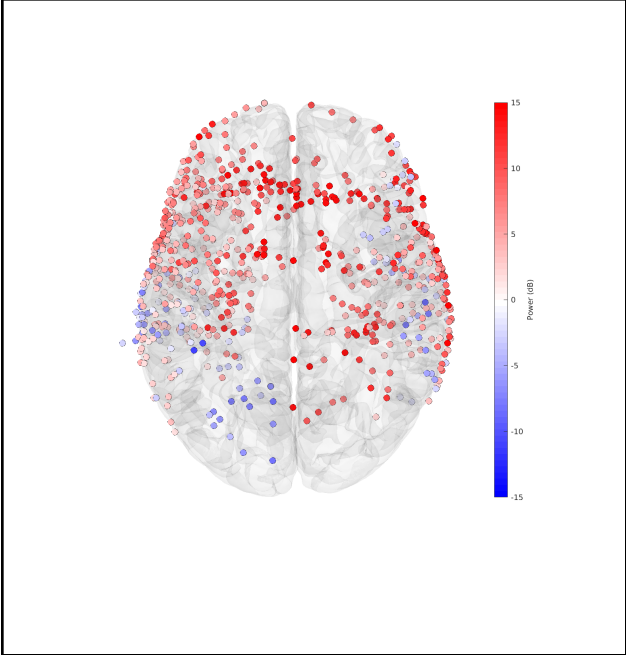


Supplementary Figure 3. Alpha power changes across channels.

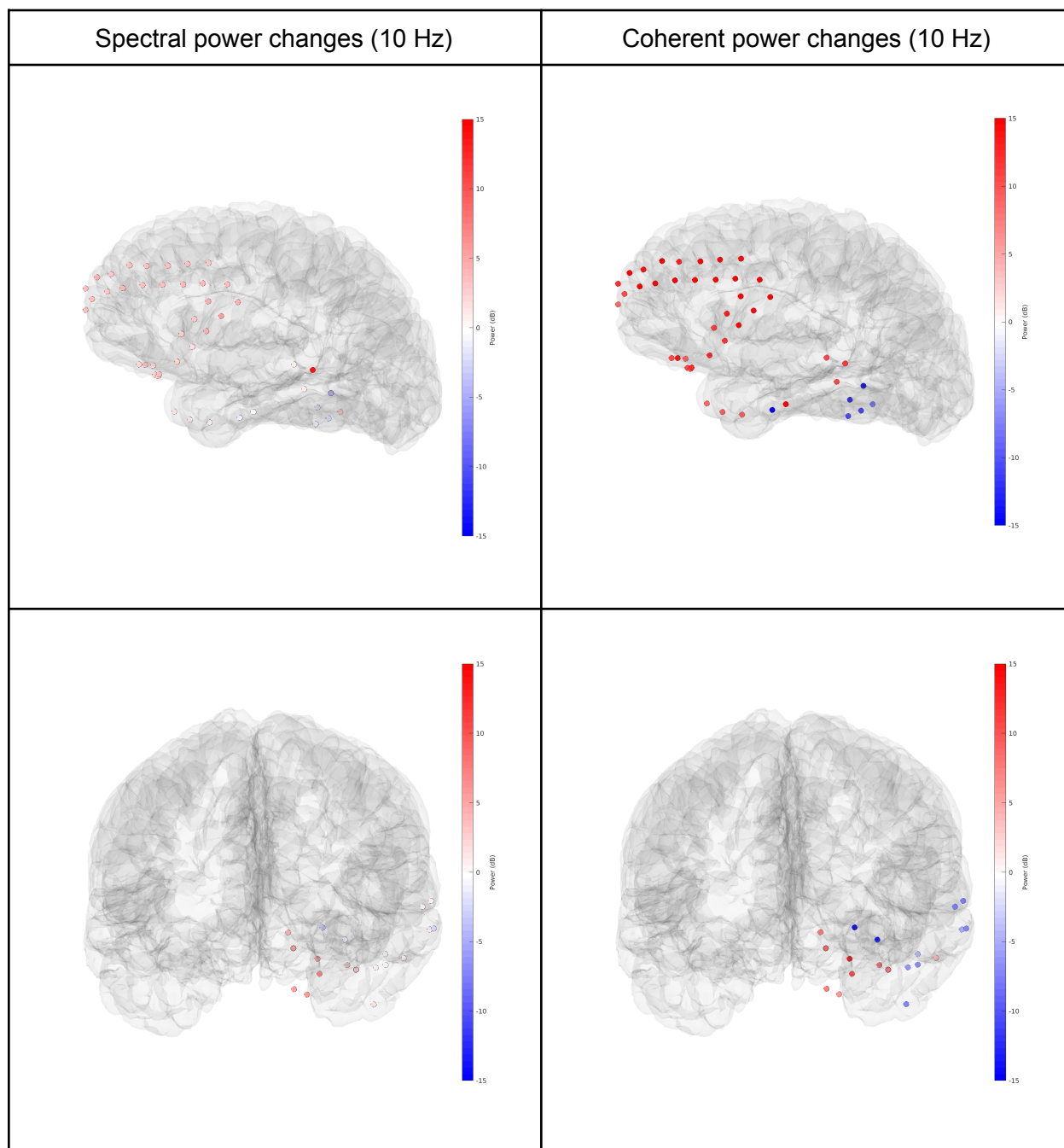
(a) Channel-wise alpha (10 Hz) multitaper spectral (left) and coherent (right) power changes between pre-LOC and post-LOC epochs from all channels in dataset, plotted in an average template brain in coronal (top), transverse (middle), and sagittal (bottom) views. Color intensities represent median bootstrap differences (similar to Figs. 2a-c) between 10-Hz multitaper spectral power in each epoch (post minus pre). (b) Channel-wise power changes in individual subjects. Each row depicts a unique subject among S1 to S11 in descending order.

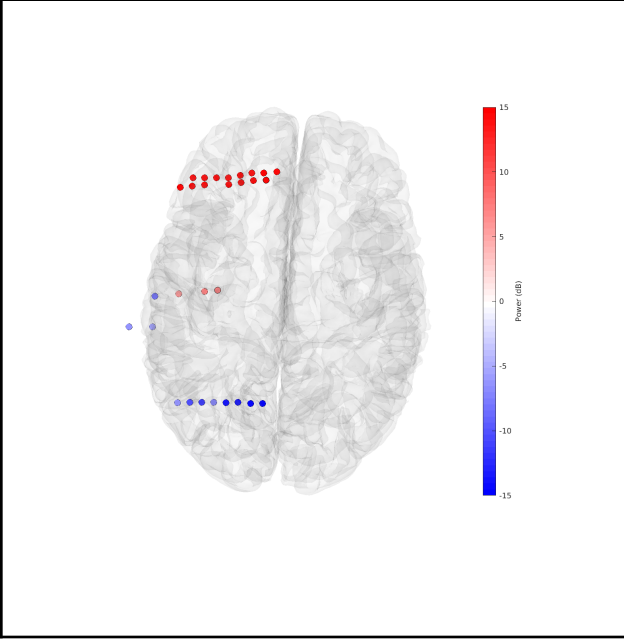
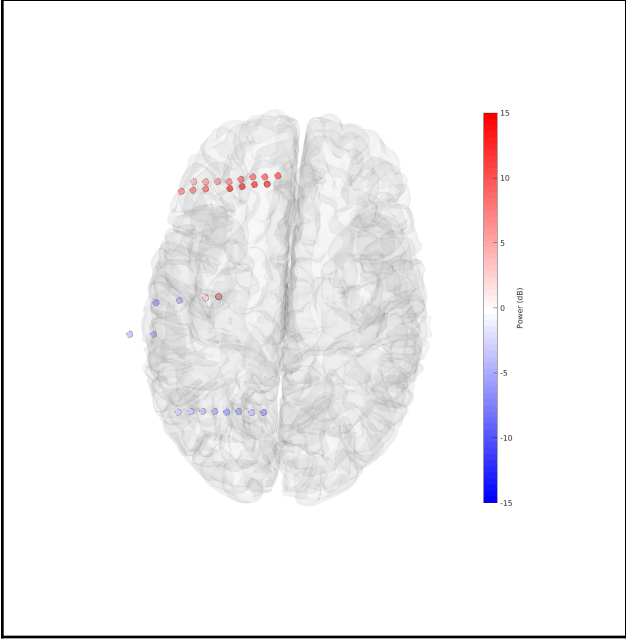
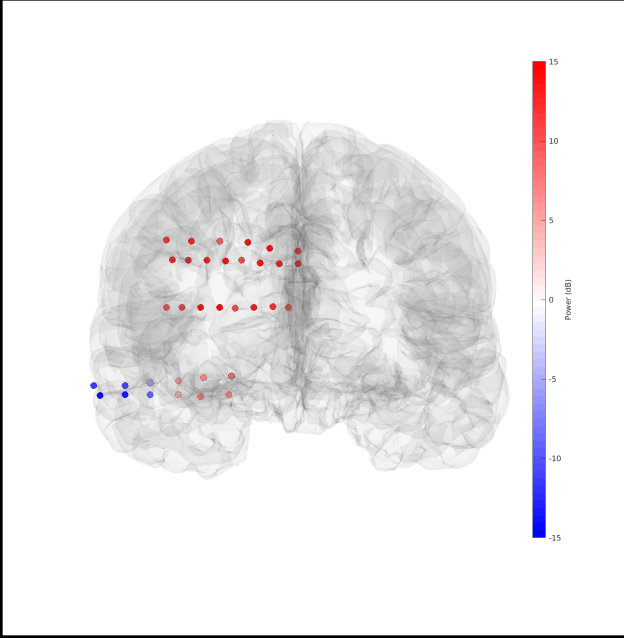
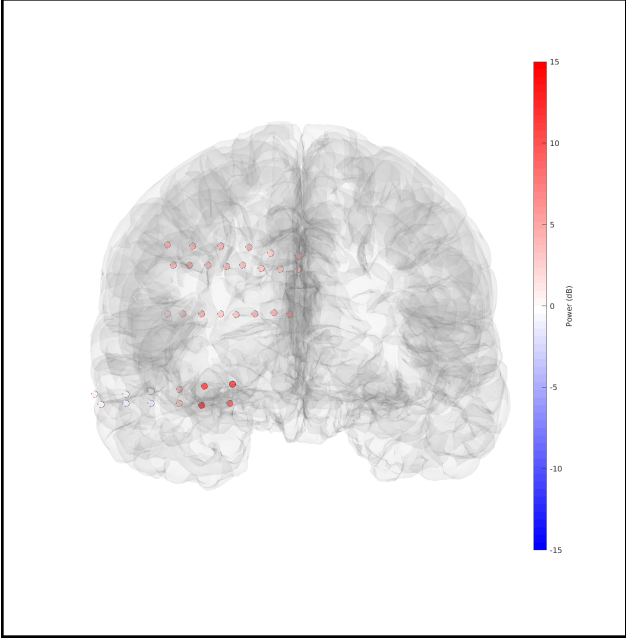
a)

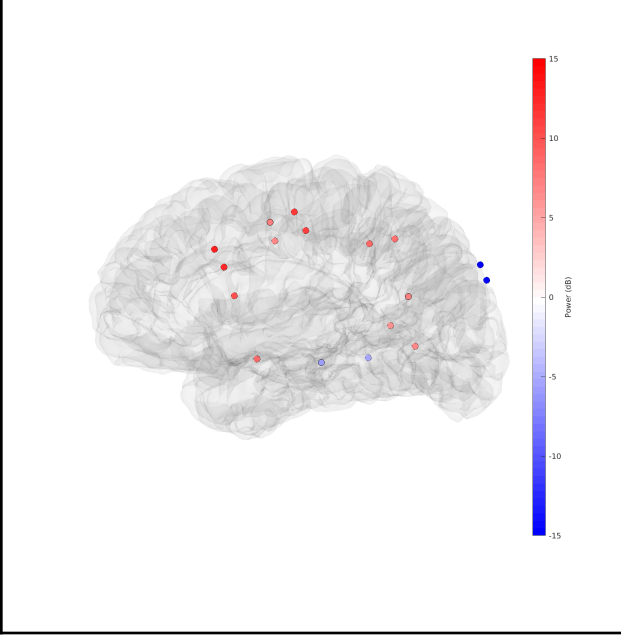
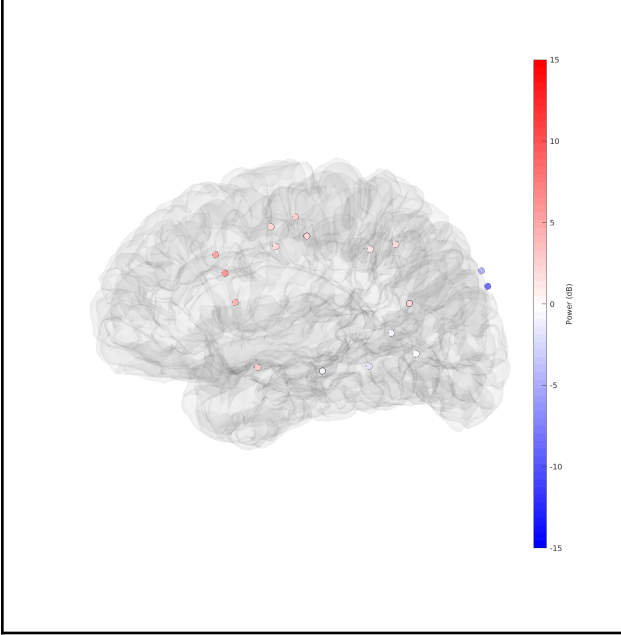
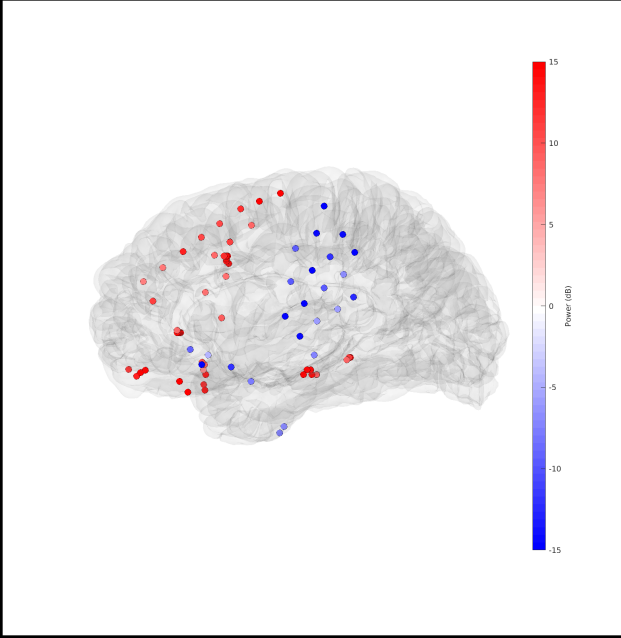
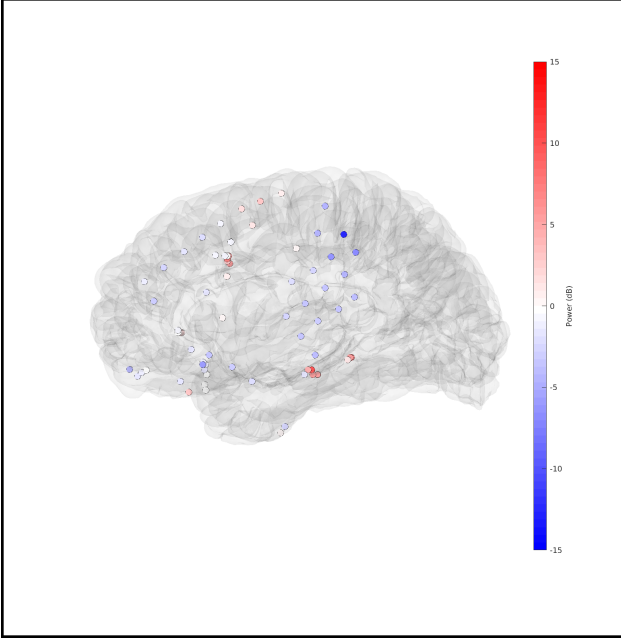


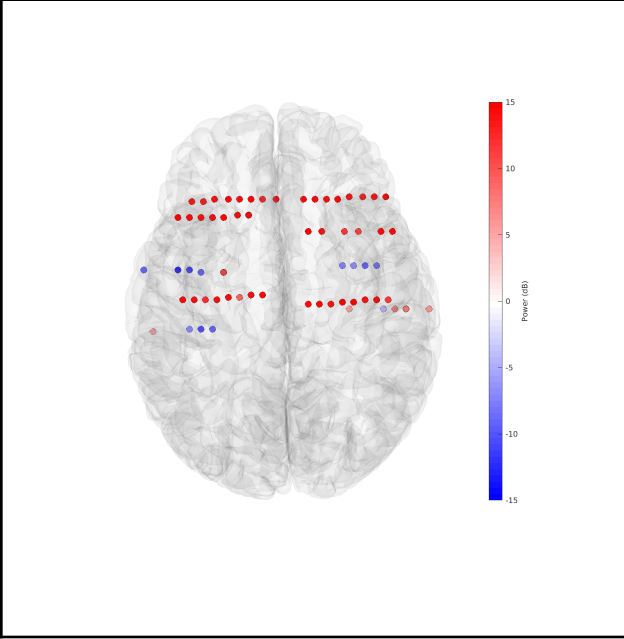
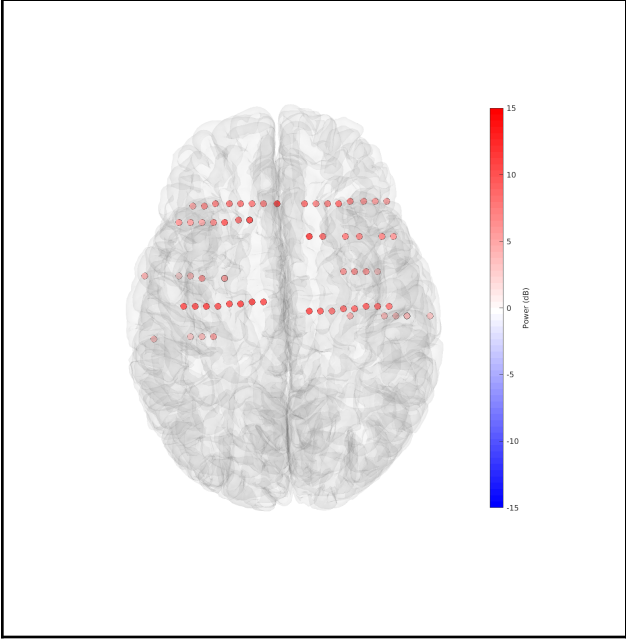
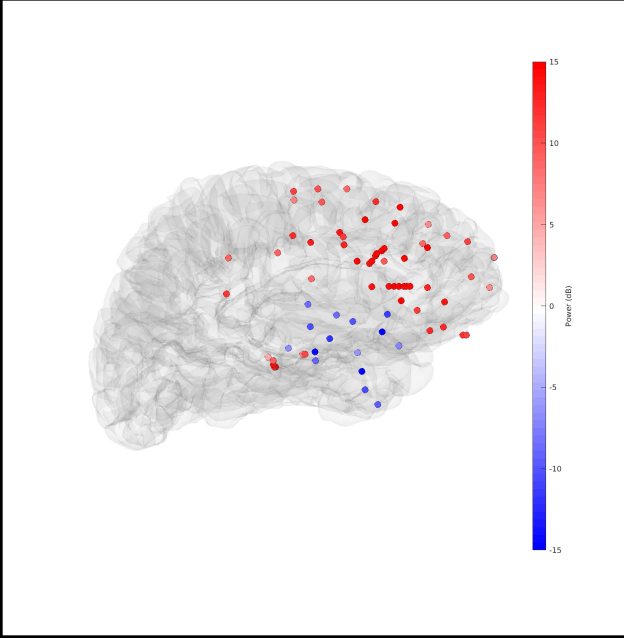
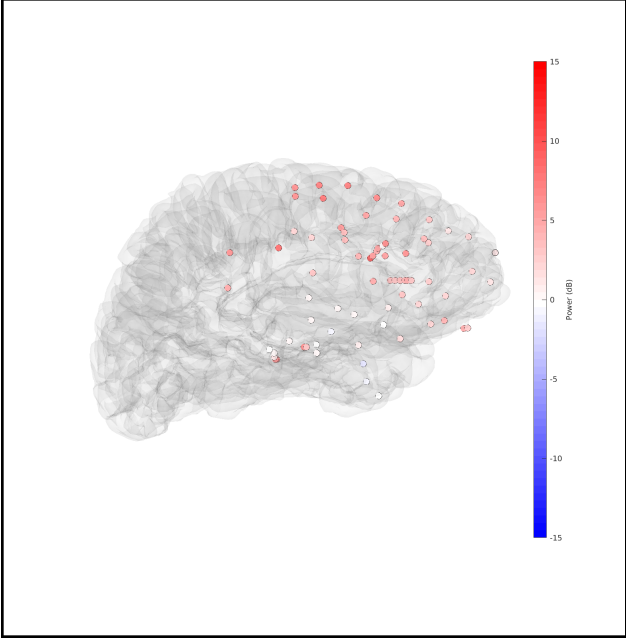


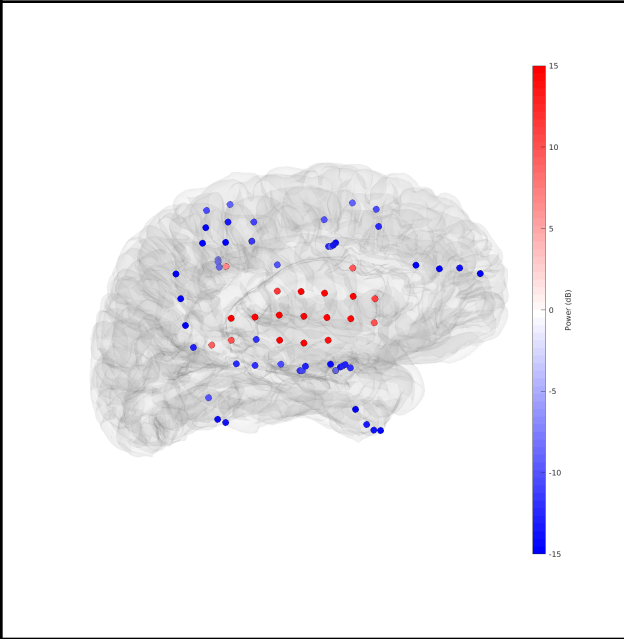
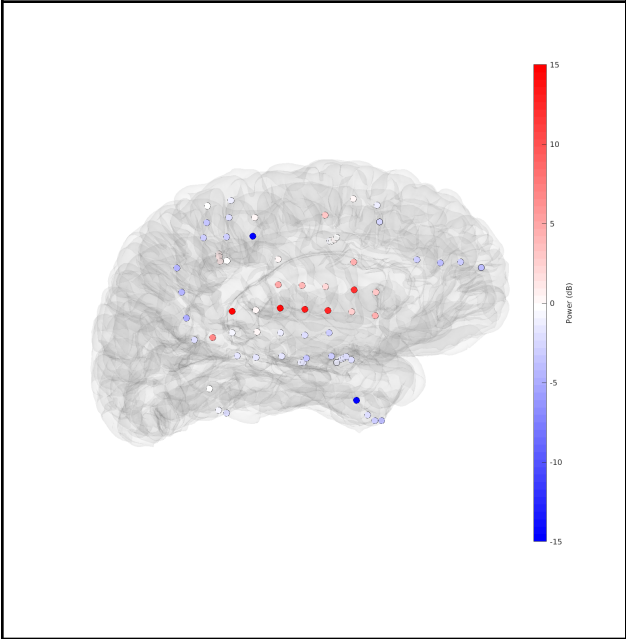
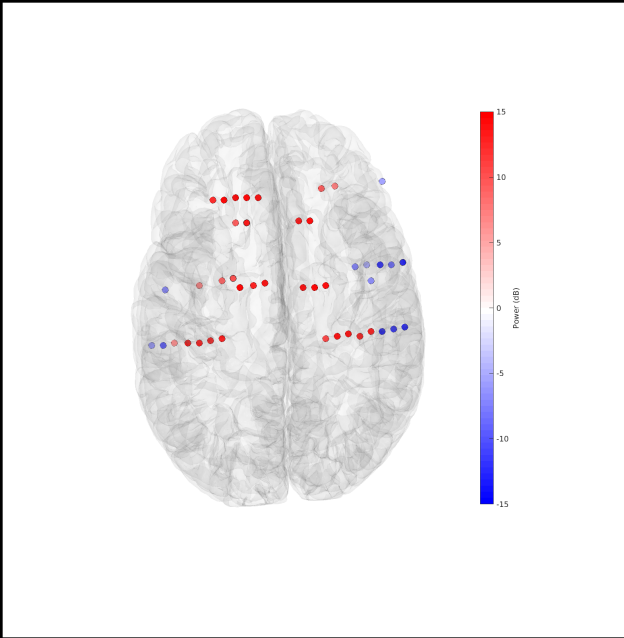
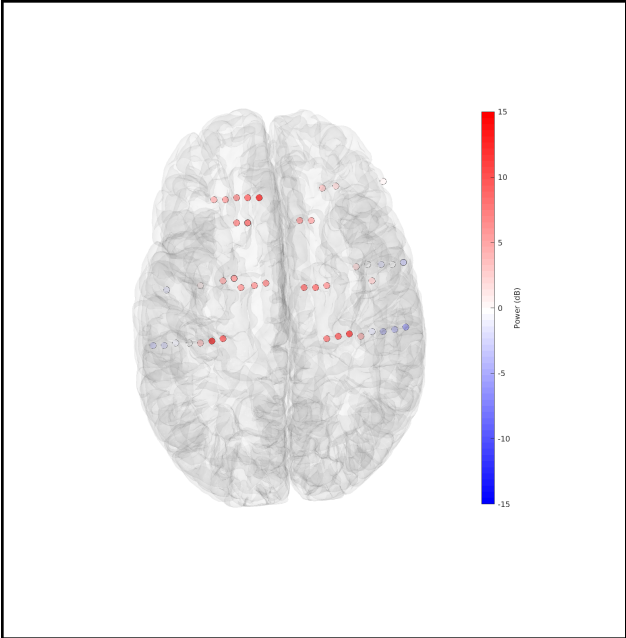
b)

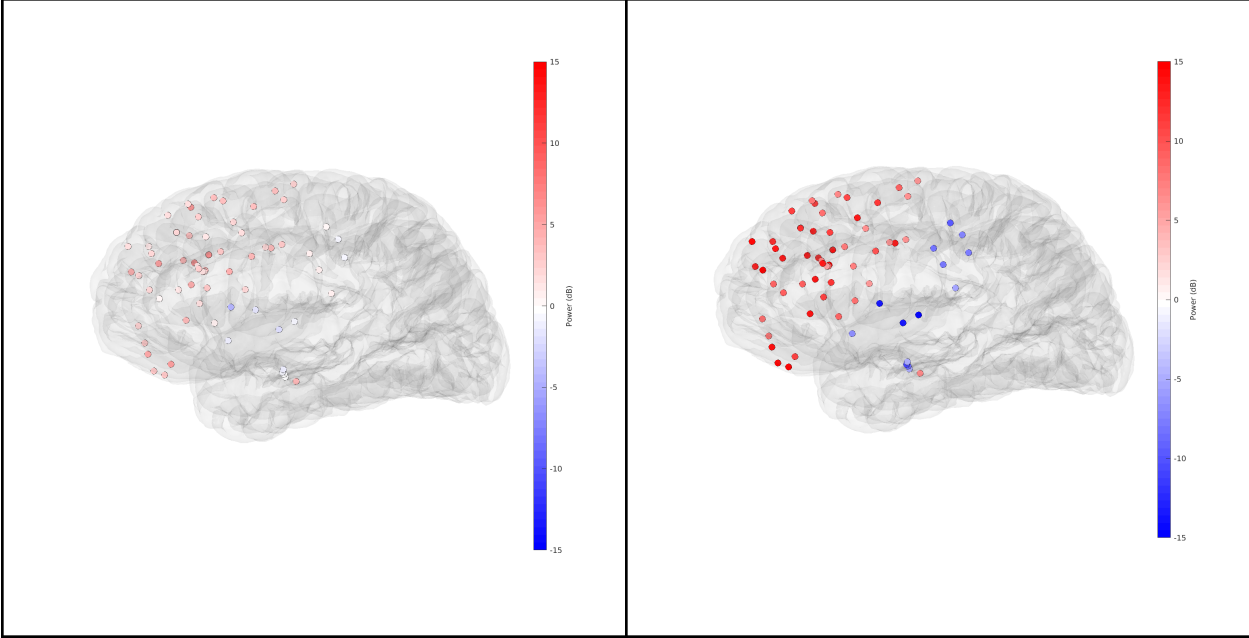






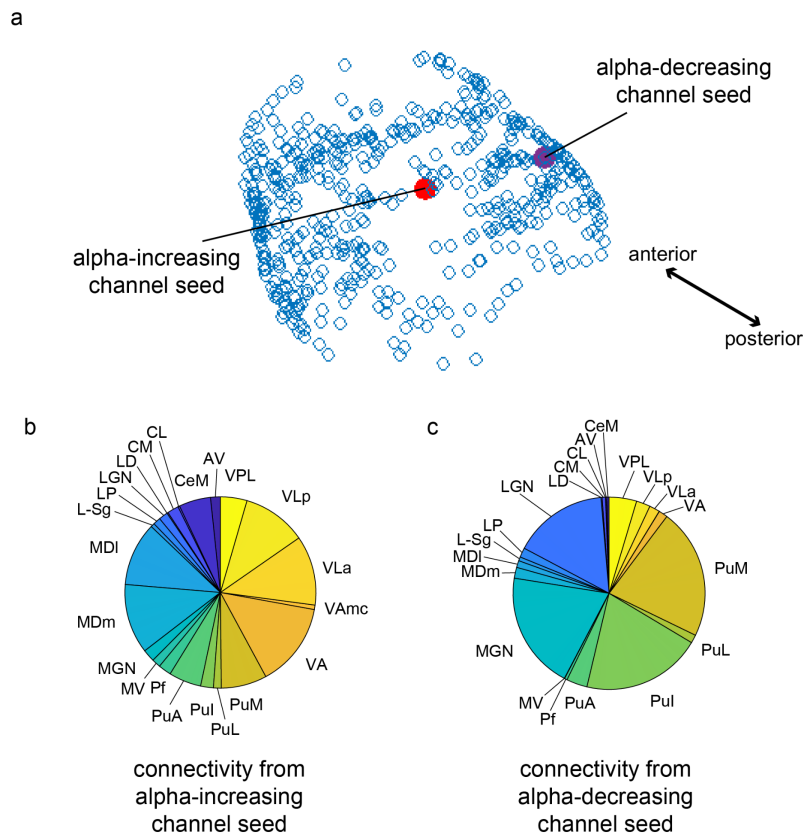






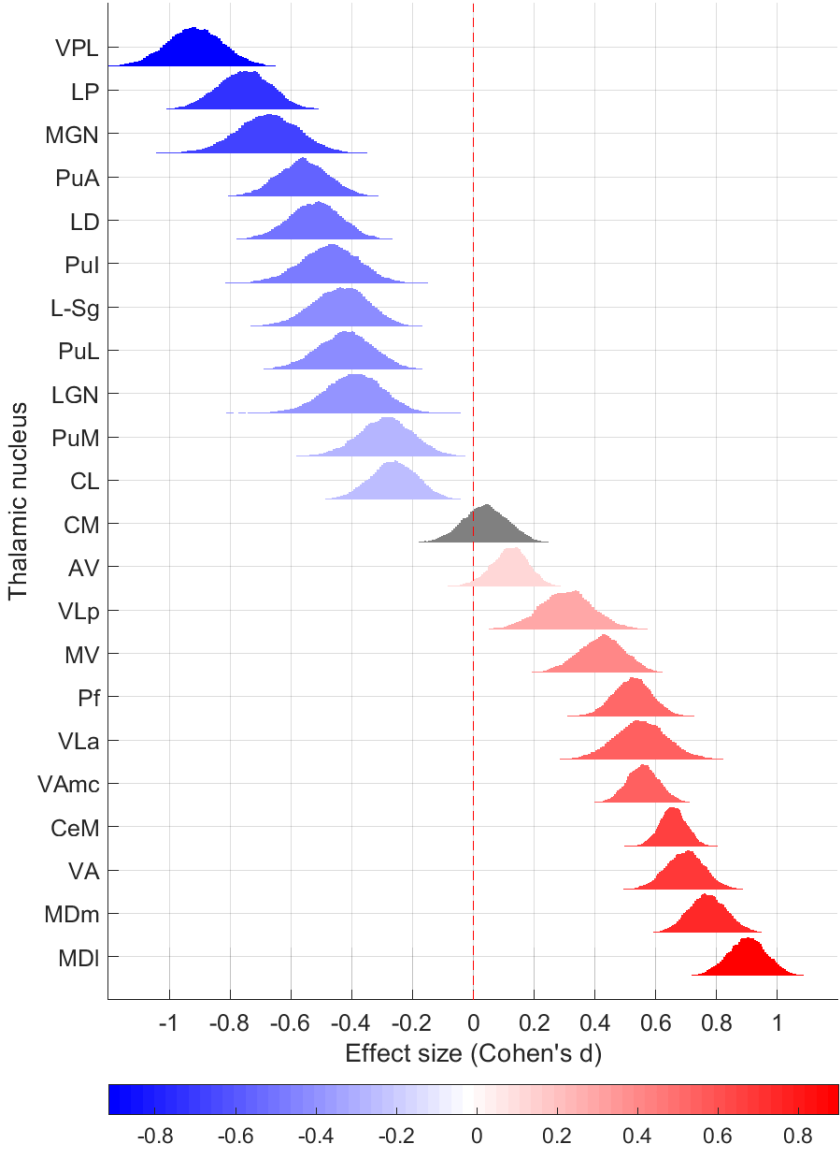
Supplementary Figure 4. Connectivity from single exemplars of alpha-increasing and -decreasing channels.

(a) Two channels were chosen from alpha-increasing and alpha-decreasing channels as depicted in Figure 2. (b, c) Pie charts depict proportion of destinations among streamlines (total $n = 10,000$) ending in the thalamus. Thalamic nucleus abbreviations: PuL = lateral pulvinar, LGN = lateral geniculate nucleus, VPL = ventral posterolateral, L-Sg = limitans-suprageniculate, PuA = anterior pulvinar, Pul = inferior pulvinar, MGN = medial geniculate nucleus, LP = lateral posterior, LD = laterodorsal, PuM = medial pulvinar, CM = centromedian, CL = central lateral, AV = anteroventral, Pf = parafascicular, VLp = posterior ventral lateral, VLa = anterior ventral lateral, MV = reuniens (medial ventral), CeM = central medial, VAmc = magnocellular ventral anterior, VA = ventral anterior, MDI = parvocellular lateral mediodorsal, MDm = magnocellular medial mediodorsal.



Supplementary Figure 5. Connectivity preference under ipsilateral tractography constraints.

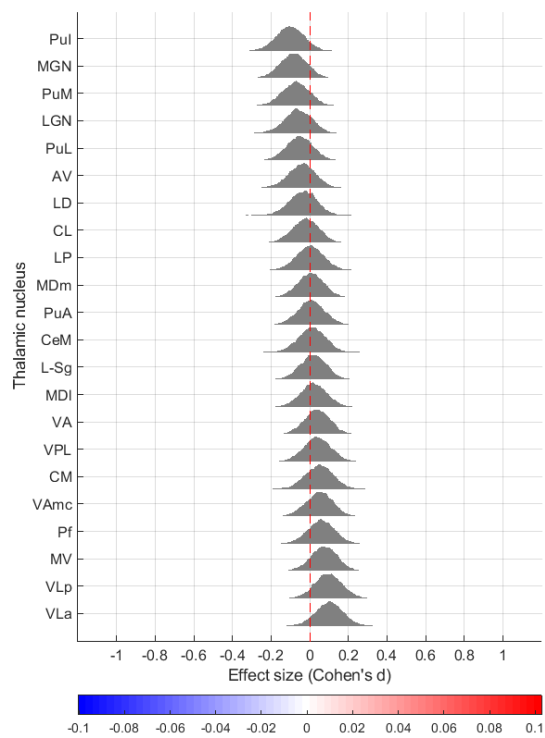
Re-analysis of preferential connectivity of thalamic nuclei to alpha-increasing and -decreasing regions (Fig. 4b) using ipsilateral cortex-to-thalamus streamlines only. Gray denotes nuclei where zero effect size was within the 95% confidence interval. (See *Methods*.)



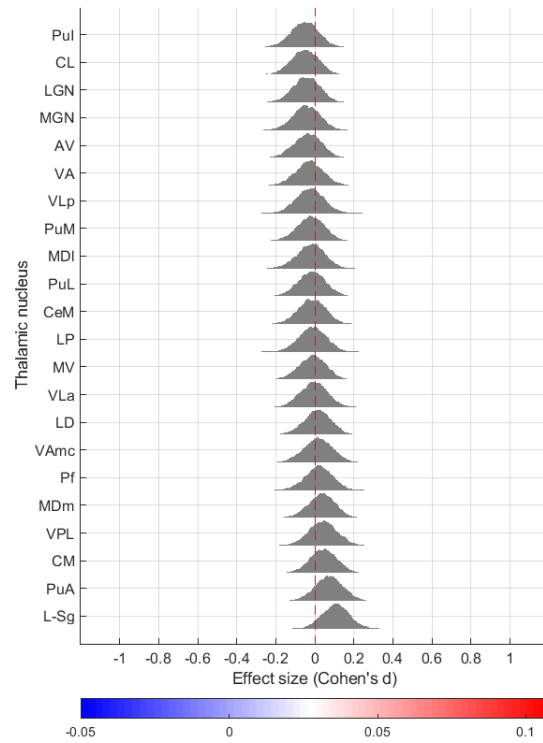
Supplementary Figure 6. Connectivity preference under null conditions.

Preferential connectivity of thalamic nuclei to two reshuffled groups of regions. Analysis was performed under settings where contralateral tracts were allowed (a) and not allowed (b), as in the preceding figure. Gray denotes nuclei where zero effect size was within the 95% confidence interval.

a)



b)



Data Materials and Availability

Diffusion-weighted imaging data used in this study is publicly available at <https://www.humanconnectome.org/study/hcp-young-adult>. Code and data will be made available in a public repository prior to publication.